Electrical Treeing in Fluoropolymer Cable Insulation

Torbjørn Andersen Ve, Hilde Marie Syvertsen, Nina Marie Thomsen,
Marit-Helen Ese, Emre Kantar and Sverre Hvidsten.

***Abstract*—This paper examines the electrical treeing phenomenon in fluoropolymers under AC voltage. A specialised test setup was designed to evaluate two distinct fluoropolymers, fluorinated ethylene propylene (FEP) and perfluoroalkoxy alkane (PFA), with cross-linked polyethylene (XLPE) serving as the reference material, given its well-documented AC treeing characteristics. Tree growth in both fluoropolymers were found to follow a somewhat classical three-stage pattern, developing bush-like trees with insulating channels. In XLPE at the same growth voltage the trees were bush-branched with a higher propagation rate than in FEP and PFA. The lower propagation rate in fluoropolymers is likely related to the higher bond strength of the carbon-fluorine bonds compared to the carbon-hydrogen bonds in XLPE. Breakdown in the materials produced indications of carbonisation products in the breakdown channel.**

***Index terms*—Electrical treeing, fluoropolymers, cable insulation.**

I. Introduction

Electrical power cable insulation systems commonly used today are different types of cross-linked polyethylene (XLPE) and ethylene propylene rubbers (EPR). Many decades of service experience and developments have resulted in high cleanliness and long lifetimes of these polymers under different conditions. However, the maximum continuous service temperature is 90 °C, which limits the applicability of the insulation types and calls for high-temperature extrudable material alternatives. This could include silicone rubbers but also extrudable fluoropolymers that have been used in different high-temperature applications where power cables are needed [1].

Electrical treeing is a major pre-breakdown mechanism in high voltage extruded cable insulation. An electrical tree consists of permanent hollow tubules or channels that develop in the polymer matrix when it is subjected to very high electrical stresses. Trees initiate in regions of very high electric fields, such as at sharp conducting protrusions at cable screen surfaces or contaminations. The initiation of trees occurs due to charge injection into the polymer and depends upon the presence of defects or electron injector materials such as metals. In general, initiation occurs due to electric stress degradation of the insulation forming a cavity where discharges can occur, or, if the electric stress is very high, due to electron avalanches breaking down the insulation [2]. When initiated, there are two mechanisms for tree propagation. In the first, partial discharge (PD) activity elongates the channels by breaking polymer bonds in the tip region of the "branches" of the tree, through processes such as auto-oxidation, the penning effect, fast electrons and/or electromechanical stress [2], [3]. In the second, the channel grows through strains produced due to either high gaseous pressure within the channels or strong electromechanical/Maxwell forces inducing cracks within the insulation, creating a continuation of the tree structure [4]. The difference between the mechanisms for initiation, and also for propagation, means that the relation between the onset of PD activity and initiation or propagation of a tree may indicate which mechanism is dominant in a system.

Until recently, there have been very few references in the literature concerning the fundamental dielectric phenomena in fluoropolymers related to high-voltage cable application. There have been a series of articles concerning DC cable applications focusing on space charge, conduction, partial discharge at DC voltage, and degradation during arcing [5], [6], [7]. While electrical treeing phenomena in XLPE are well known (see e.g. [2], [8]), treeing in fluoropolymers is not much covered by literature. The main purpose of this paper has been to study AC electrical treeing in two fluoropolymers; fluorinated ethylene propylene (FEP) and perfluoroalkoxy alkane (PFA), using a new setup design with no need for submerging samples in insulating oil during experiments.

This work is funded by the project “High Temperature Subsea Power Cables” (HiTCab), supported by the following industrial partners: Habia Cable AB, Equinor Energy AS, AGC Chemicals Europe, Subsea7 Norway AS, Technip Norge AS, Neptune Energy Norge AS, Conocophillips Skandinavia AS, Chevron Technical Center (a division of Chevron U.S.A. Inc.), Axon Cable SAS and Daikin Europe GmbH.

Torbjørn Andersen Ve (e-mail: torbjornandersen.ve@sintef.no), Hilde Marie Syvertsen, Nina Marie Thomsen, Marit Helen Ese, Emre Kantar and Sverre Hvidsten are all with SINTEF Energi AS, NO-7465, Norway.

II. Methods and Materials

A. Electrical Treeing Experiments at High Temperatures

Traditionally electrical treeing experiments are performed with the sample submerged in an insulating oil to avoid spurious discharges at the surface of the polymer. The setup used in this paper is designed to facilitate experiments at high temperatures where oil absorption by the sample during the test could likely influence the results. The absorption of liquids in polymers is temperature dependent, and both the maximum amount absorbed, and rate of absorption increase strongly with temperature. It is expected that absorption of oil will fill the free volume in the polymer, which has been shown to increase electrical tree initiation voltage [9]. Any micro-voids may also be filled if high enough amounts of oil are absorbed after sufficient time of exposure. Removing the oil eliminates the absorption issues but introduces the risk of surface ionisation and discharges on the sample surface near the needle. Although surface discharges would not affect tree growth, they would limit the sensitivity of PD measurements through the noise they generate and make PD analysis challenging. Surface discharges are challenging to mitigate, as while increasing the sample's thickness can reduce the electric field at the surface, diminishing the risk of surface discharge, it might also compromise the sample's transparency. With optical microscopy as the main measurement technique for tree growth, an opaque sample is not desired. The electrode setup was therefore optimised in COMSOL Multiphysics to find a compromise between the transparency of the sample and the surface discharge mitigation. This was done by embedding the high voltage and ground electrodes and adding geometric field grading electrodes to obtain an as thin-as-possible sample while limiting the electric field in air to less than 2.6 kV/mm at 15 kV. This was done to minimise the chance of surface discharges [10] at the expected maximum voltage in the setup. To verify that the setup was PD free at the desired voltages, PD measurements were performed after the setup was constructed, both without samples and with dummy samples with a larger gap distance, at voltages up to 15 kV with no significant PD activity detected.

B. Materials, Electrodes and Sample Geometry

The needle-plane test objects were made from three different materials: the fluoropolymers FEP and PFA, and the reference XLPE. A test object consisted of the embedded ground electrode, the needle high voltage electrode, and the polymer insulation cast around the electrodes. Input from the COMSOL

TABLE I
Compression Moulding Specifications for Each Polymer Material.

	XLPE	PFA	FEP
Low pressure	120 °C 10 min (2.9 MPa)	330 °C 30 min (0 MPa)	290 °C 30 min (1.8 MPa)
High pressure	175 °C 30 min (18 MPa)	330 °C 1.5 min (7.2 MPa)	260 °C 2 min (7.2 MPa)

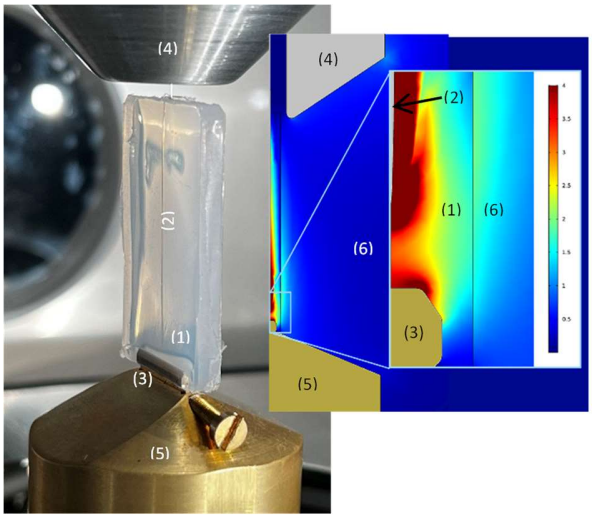

Fig. 1. Image of the polymer sample mounted in the test setup, and a COMSOL model with inset zoomed on the needle-ground gap. (1) Polymer sample. (2) Needle at high voltage. (3) Embedded ground electrode. (4) High voltage field grading electrode. (5) Ground field grading electrode. (6) Air

models were used as a basis when manufacturing the electrodes, as can be seen in Fig. 1. Acupuncture stainless steel needles were used as high voltage electrodes. The electrode diameter was 300 µm, with a tip radius of less than 0.5 µm. Samples had a thickness of 4 mm and a default gap distance of 2 mm between the needle tip and the ground electrode. In the setup both the needle and the embedded ground electrode were connected to larger electrodes graded away from the gap to limit the electric field.

To produce a test object, polymer pellets of XLPE were extruded into thin tape, which were then cut up and casted into 2 mm plates. PFA was delivered as 2 mm plates by the supplier. Whereas FEP was delivered as pellets which could be directly cast into 2 mm plates. Pre-shaped polymer parts were manufactured from the plates, using a custom-made hole-punching tool, and two parts used to make one complete test object. One pre-shaped polymer part was placed on either side of the needle and ground electrode and compression moulded into the final test object. The temperature, duration and pressure settings during the compression moulding were optimised for each of the materials and are presented in Table I. The samples were first heated in the moulds at low pressure, after which the pressure was increased to ensure minimise the risk of gas bubbles or cavities remaining in the samples after compression moulding. 0 MPa for PFA means that the hydraulic press plates were moved into contact with the moulds but no additional pressure was applied. All sample preparation work was carried out in HEPA filtered air environments to prevent contamination of the samples. Samples were only removed from the filtered air environment when sealed in moulds.

C. Experimental Setup and Electrical Treeing Procedure

The experimental setup is shown in Fig. 2. The sample was mounted in the electrode system, connected through a 50 mΩ

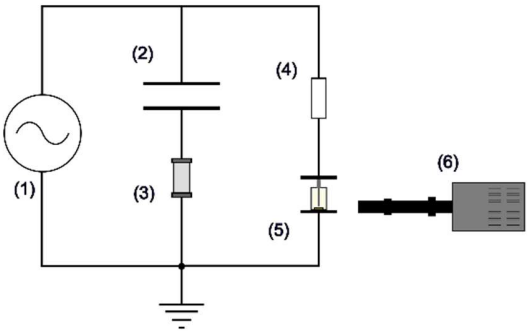

Fig. 2. Experimental setup for electrical treeing. (1) High voltage AC source. (2) Coupling capacitor. (3) PD measurement system. (4) Current limiting resistor. (5) Sample and electrode system. (6) Camera with long-distance microscope.

current limiting resistor to a high voltage 110 kV AC source. An 800 pF coupling capacitor was connected in parallel to the sample and coupled the signal to a commercial PD measurement system. A camera equipped with a long-distance microscope recorded the tree growth.

Prior to the electrical tree growth studies, a short electrical tree was incepted using a pre-defined voltage step procedure: Starting at a voltage of 5 kV, the voltage was increased by 1 kV every 5 minutes until treeing occurred. At 10 kV, the step duration was increased to 10 minutes, and at 15 kV to 15 minutes, if necessary, to allow more time for a tree to initiate at each step. In general, most trees initiated at less than 10 kV. Tree initiation was stopped when a tree was detected using the camera or when significant PD activity was detected. Most often, tree initiation was detected on the camera. To ensure the highest sensitivity, around 0.5 pC, during the PD measurements, the current limiting resistor was removed during this stage.

When tree initiation was detected, the sample was removed, and the initial tree length measured using a microscope. The sample was then re-mounted in the electrical treeing setup, and the growth procedure started.

Tree growth was performed at 10 kV applied voltage. To preserve the sample and measurement setup in case of breakdown during this part of the experiment, the current limiting resistor was placed between the high voltage source and the sample, as shown in Fig. 2. During the growth stage, PD activity was monitored continuously, and images of the gap where the tree growth occurs were taken every 3 seconds. This stage continued until the tree had bridged approximately 80 % of the gap distance, or in a few cases until breakdown occurred.

D. Chemical Composition Analysis of Breakdown Channels

The chemical composition of the black breakdown channels observed after electrical treeing in all three materials, were investigated using Raman spectroscopy. Firstly, the samples were cut by a manual microtome giving approximately 300 µm thick slices. The samples were cut along the tree channels leaving the black branches exposed. Raman spectra were recorded using a Raman imaging microscope with a monochromatic diode laser (532 nm wavelength). A laser power of 5-10 mW was used with an integration time of 10 seconds.

III. Experimental Results and Discussion

A. Initiation of Electrical Trees

Table II shows the initiation times and voltages for the three different materials. As can be seen from the table, both fluoropolymers appear to have a longer initiation time than XLPE. In XLPE, trees were initiated in less than 10 minutes, with all trees initiating in the voltage range of 5-7 kV. For FEP, trees were initiated at 8 kV or above, with several samples exceeding 10 kV during the initiation stage. This indicates that FEP may be more resistive to tree initiation than XLPE. This is likely due to a difference in polymer bond strength – carbon-fluorine bonds have a higher bond strength than carbon-hydrogen bonds [11], and the presence of fluorine also slightly increases the bond strength of the carbon chain itself [12]. Given that the autooxidation initiation mechanism is dependent upon the creation of radicals through bond breaking, it seems likely that this increases tree initiation time and voltage for FEP compared to XLPE. Relatedly, FEP has been found to not oxidise with only thermal ageing stress at temperatures up to 140 °C [13]. For PFA, however, the tree initiation times were scattered: while one tree was initiated already at 6 kV in one sample, no tree initiation occurred in another sample until at 15 kV applied voltage. The differences in initiation time might be related to the adhesion between needle and polymer after sample production, where poor adhesion would create a void where PD activity would occur. It is also likely that the PFA

TABLE II.
Tree Initiation Times, Initiation Voltages, and Initial Tree Lengths.

	XLPE			FEP			PFA		
Sample	Initiation time [min]	Initiation voltage [kV]	Initial tree length [µm]	Initiation time [min]	Initiation voltage [kV]	Initial tree length [µm]	Initiation time [min]	Initiation voltage [kV]	Initial tree length [µm]
1	10	7	70	55	12	322	77	15	428
2	5	6	97	20	8	79	18	8	121
3	2	5	102	> 80	15	174	5	6	43
4	3	5	40	39	11	349	11	7	101
5	5	6	67	27	10	291	17	8	80

samples experienced a greater difference in thermal expansion and contraction between the polymer and the needle than the two other materials, due to the higher processing temperature. In case of a void at the needle tip, it might be expected that the PD activity would be observed prior to the initiation of a tree. However, for most samples, this was not the case. Only one of the XLPE samples and one of the FEP samples exhibited detectable PD activity before a tree was observed. None of the PFA samples showed such activity. For both the XLPE and the FEP sample that showed PD activity prior to tree initiation, PD did not start immediately as voltage was applied; in fact, the FEP sample in question was FEP_3, which had the longest initiation time out of all tested samples.

B. Propagation of Electrical Trees

Fig. 3, 4 and 5 show the growth of the tree as a function of time for the different materials. For all samples, the tree growth was started from an initiated tree of various lengths. For some samples, the initial tree spanned a significant part of the gap distance, e.g. for PFA_1 the initial tree was 20 % of the gap. This was in general connected to the voltage needed to initiate a tree – the tree growth rate is significantly higher at higher voltages, and the initial tree therefore grows longer before the voltage is manually switched off during initiation.

Tree growth for XLPE was relatively uniform, with trees growing at a near-constant rate. On average, XLPE had the highest growth rate, around 100 µm/min, although there was significant variation between the samples; the slowest growing on average 50 µm/min and the fastest around 200 µm/min.

For FEP, two samples exhibited a near-constant growth rate, while three showed an initial period of more rapid growth, followed by a period of slower growth. Two of those also had a final rapid growth phase. The slow-growth phase led to almost a pause in the growth for two samples, growing around 2 µm/min, compared to the average growth rate of between 20 to 40 µm/min for the initial phase of those samples. The overall average growth rate for FEP was around 40 µm/mm, varying between 8-70 µm/min.

As can be seen in Fig. 3, 4 and 5 the tree growth in FEP on average is slower than in XLPE. As mentioned in Section IIIA, this may be related to a higher bond strength of the polymer chain of FEP compared to XLPE.

Tree propagation in PFA was similar to FEP, as three samples exhibited steady growth, while two samples had an initial period of rapid growth followed by a slower growth period. The propagation rates were in-between XLPE and FEP, varying between 40-130 µm/min, with an average propagation rate of 80 µm/min.

C. Tree Morphology

Microscope images of the tree after one minute of growth and one minute before breakdown are shown in Fig. 6 for each material. All materials exhibited fairly wide trees, with the width of the tree being at least 50 % of its length. While using samples consisting of two pre-shaped parts joined together during compression moulding may increase the risk that trees grow only in the plane where the two parts are joined, this

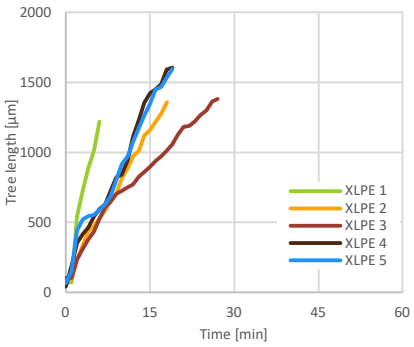

Fig. 3. Electrical tree propagation in XLPE.

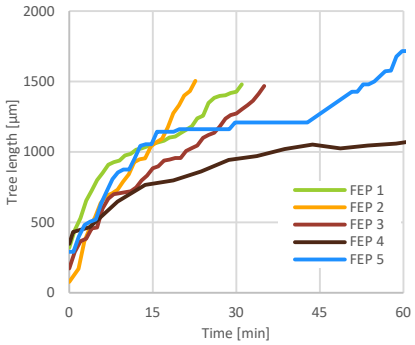

Fig. 4. Electrical tree propagation in FEP.

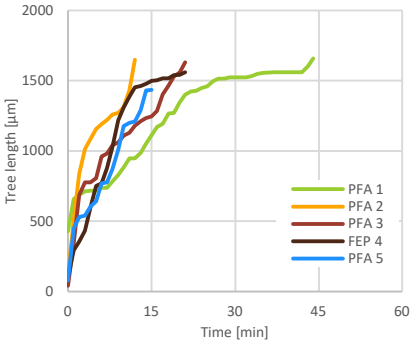

Fig. 5. Electrical tree propagation in PFA.

appears not to be the case as the three-dimensional tree growth, including tree channels and breakdown channels, did not show any bias towards any specific plane. The growth in general started from the needle tip closest to the ground electrode, grew for a short time, some tens of seconds up to two minutes, towards ground, and then started branching, growing wider over time. This fits the three-stage model for tree growth, with a more rapid stage, a slightly slower main growth stage that may have a partial stagnation phase, and a more rapid growth stage, often called the runaway stage, towards the end. Comparing this with what has been observed in literature, they could all be categorised as branch-bush or bush-like trees. [8]

In XLPE, trees grew to a branchy bush-like structure, with channels growing side-branches even at the later stages of tree growth. This corresponds to the type of trees found at higher electric field strengths [8]. In a typical XLPE tree, a high number of distinguishable branches grew at approximately the

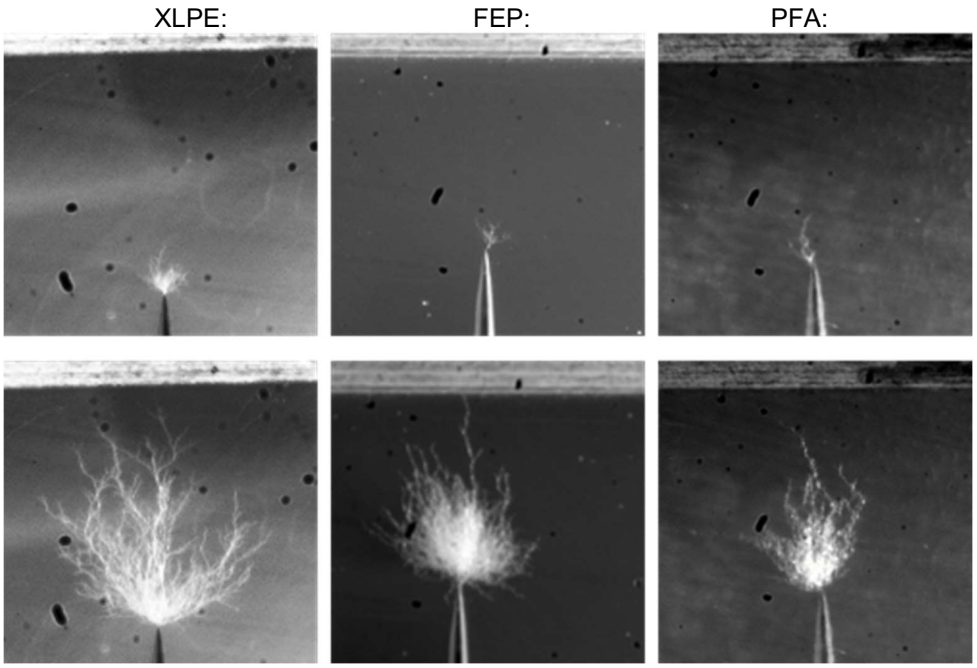

Fig. 6. Examples of electrical tree structures in XLPE, FEP and PFA, 1 minute into the growth period (upper row) and 1 minute before breakdown (lower row). Black dots are artefacts on the camera sensor chip.

same rate until just before breakdown. In the final stage only one single branch grew rapidly to reach the ground electrode, corresponding to the runaway stage of tree growth. The trees were more branch-like than FEP and PFA, and did not exhibit a stagnation phase. This is very close to what has been observed previously for XLPE with similar gap distances and voltages [14].

For FEP, the growth was slightly different; the trees were more bush-like in appearance. Comparing this to what has been observed in XLPE, this tree growth type would be expected to occur at lower electrical fields than bush-branched trees [8]. The tree growth towards the ground electrode often stagnated, while the channel density near the needle tip increased with time. As can be seen in Fig. 7, this was both due to the channel near the needle tip widening and due to new channels being formed in the bulk of the tree. The stagnation in tree growth observed in Fig. 4 was therefore not a pause in overall tree channel growth, just a pause in the growth of the lead channels. The simultaneous reduction in growth rate and continued increase in channel density, often referred to as fractalization, have also been observed in XLPE previously [14], [15]. The increase in tree growth rate observed later in the growth stage was often caused by a single channel starting to grow towards the ground electrode again; this corresponds to the runaway stage of tree growth [8].

The trees in PFA were narrower and slightly more branchy than those observed in FEP. In two of the samples, a reduction in growth rate was caused by the leading branch having stopped growing, while one or several other shorter branches throughout the tree started to extend towards the ground electrode. For PFA, there was also densification of the bulk tree structure, with new channels being formed in the tree structure. This is similar to what occurred in FEP.

D. Partial Discharges

Fig. 8 displays a representative selection of partial discharge plots for each of the materials, comparing the partial discharge activity during the initial minute of tree growth and the final minute before the tree length covers 80 % of the gap between the needle and the ground electrode.

As can be seen in the phase resolved partial discharge (PRPD) patterns in Fig. 8, both the shape and the PD magnitude differs for the three materials. For XLPE and PFA flat turtle-

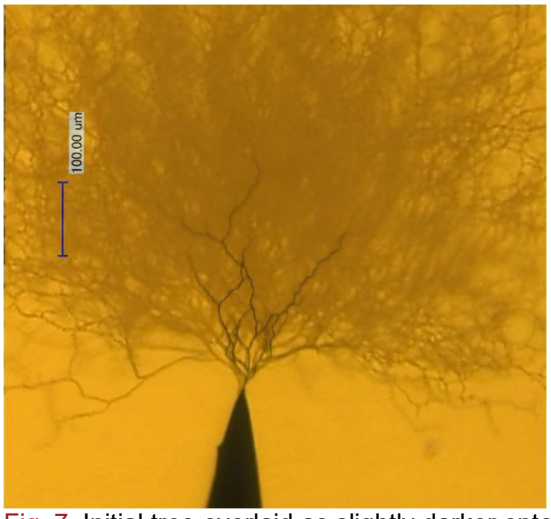

Fig. 7. Initial tree overlaid as slightly darker onto the final tree structure, sample FEP 1.

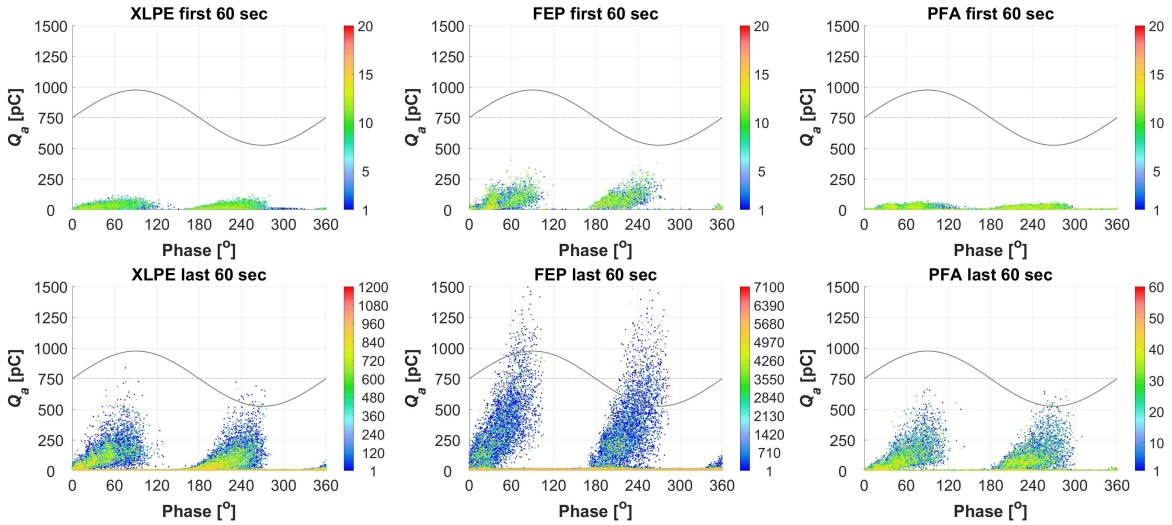

Fig. 8. Phase resolved PD plots for XLPE, FEP and PFA, during the initial minute of tree growth and the final minute before the tree length was 80% of the gap distance between the needle and the ground electrode. Note the difference in scaling of number of PDs on the lower row.

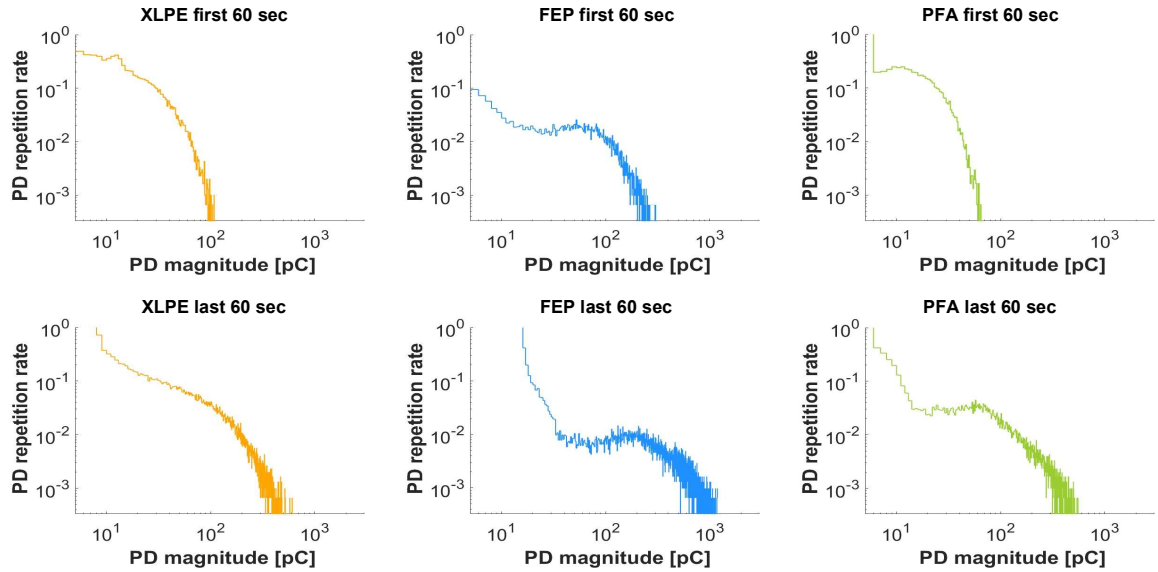

Fig. 9. Repetition rate and magnitude of PD events typical for XLPE, FEP and PFA samples, showing the first 60 seconds of tree growth and the last 60 seconds before the tree length was 80 % of the gap distance.

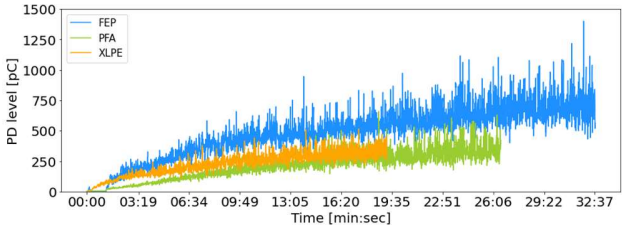

Fig. 10. PD level over time typical for XLPE, FEP and PFA.

shaped patterns are observed during the initial minute of tree growth, which is more characteristic for voids, whereas wing-like patterns, typical for electrical treeing, are observed during the final minute of tree growth [16]. The change in patterns could be due to the change in electrical tree channel length: the turtle pattern has been linked to shorter channels whereas wing-like patterns are observed in channels with greater length-to-width ratios [17].

For FEP a wing-like pattern is observed also during the initial minute of tree growth which may be explained by FEP samples having longer initial tree lengths (avg. 242 µm) compared to XLPE (avg. 75 µm) and PFA (avg. 155 µm).

When comparing the magnitude and number of PDs during the initial and final minute of tree growth, FEP achieves a significantly higher PD magnitude and activity than XLPE and PFA. As seen in Fig. 9, during the initial minute, PD events over 300 pC are recorded for FEP, whereas PFA and XLPE achieve around 70 pC and 90 pC, respectively. This could be explained by FEP having longer initial electrical trees. During the final minute of tree growth, the difference between the materials has increased further; PD events for FEP reach 1500 pC whereas PFA and XLPE achieve around 600 pC and 800 pC, respectively. During the final minute of measurements, electrical trees in all samples cover 80% of the gap distance, which indicates that PD level must also be related to other parameters than tree length.

In Fig. 10, the development of PD level over time for the three materials is compared. As can be seen, the PD activity for all three materials increases throughout the test, consistent with insulating tree channels. FEP has a higher level of PD activity throughout the entire tree growth procedure, with an initial high PD growth rate the first 10 minutes. However, the electrical tree growth in FEP samples was slower than in PFA and XLPE, and the magnitude and number of PDs seem not to be in direct relation to the electrical tree propagation towards the ground electrode. Instead, the PDs detected during electrical tree growth likely occur in the larger channels further back in the tree structure and are related to the widening of the electrical trees and channel densification observed during tree growth.

The PFA samples have the lowest magnitude of PD events, with very few events during the initial minute and a subsequent steady increase in PD level during the remaining measurement period. The PD level of XLPE is somewhere in between FEP and PFA. XLPE samples see a high PD growth rate during the first three minutes, which then stagnates during the remainder of the procedure, resulting in PD levels only marginally higher than for PFA. Overall, all three materials display a steady increase in PD with no sudden bursts of higher discharges. This has been suggested to correlate with a bushy tree structure, similar to the structures in the FEP and PFA samples and the, although somewhat more branchy, bush-like structures in XLPE [18], with the trees having insulating rather than conducting channels [14].

E. Raman Spectroscopy

For all three materials, electrical breakdown resulted in the breakdown channel turning black as it reached the ground electrode. Optical microscope images in Fig. 11 of each material show the samples' progression towards breakdown. The breakdown channel in the FEP sample appears expanded compared to the XLPE and PFA samples. The black breakdown channel in the PFA sample was less visible and appeared the least decomposed. Studies using Raman spectroscopy on XLPE cable insulation materials have shown that a black breakdown channel indicates traces of carbonaceous compounds [19], [20]. In this work, a current-limiting resistor was used, reducing the dissipated energy in the sample during the breakdown. This might be the reason why some trees showed very little signs of carbonisation.

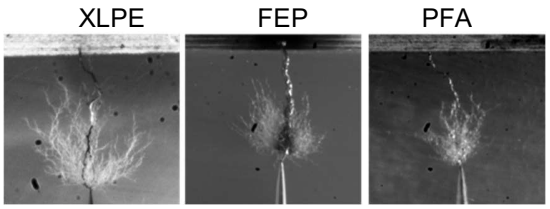

Fig. 11. Microscope images of breakdown in XLPE, FEP and PFA

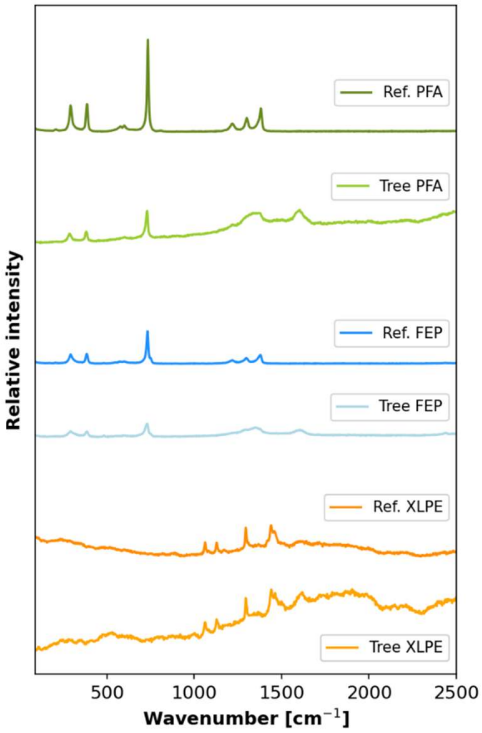

Fig. 12. Spectra recorded in the three different materials.

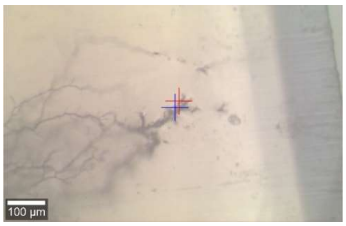

Fig. 13. Microscope image during Raman spectroscopy of an electrical tree channel in a 300 µm thick sample slice.

The resulting Raman spectra of XLPE, FEP and PFA are given in Fig. 12. Reference spectra, denoted *Ref.*, were recorded at the polymer surfaces outside of the degraded area. Tree channels, denoted *Tree*, were recorded at black areas in the tree channel structure as shown in the microscope image in Fig. 13 taken during the Raman analysis. The crosses indicate where in the sample the spectra were recorded. Broad bands from approximately 1260 cm^{-1} to 1380 cm^{-1} and 1560 cm^{-1} to 1660 cm^{-1} were observed in the spectra from breakdown channels in all three materials. The broad bands could be an indication of the D and G band of graphite or amorphous carbon as found in the previously mentioned works on XLPE. Literature states that co-polymers have shown to be more

complicated to investigate as bands might be broadened and shift position [21]. This, as well as the presence of fluorescence, makes it harder to conclusively confirm the presence and type of carbon, and a greater number of samples should be investigated to verify the results.

F. Summary

In general, both FEP and PFA showed a higher resistance to tree initiation and growth than XLPE, likely related to higher polymer chain bond strength of the former two compared to the latter. All materials had, for the most part, no detectable PD activity before tree initiation. This indicates that any pre-existing voids potentially leading to electrical tree initiation are very small, estimated to be less than 3 µm based on Paschen's law, or that for these materials the electric stress is high enough to initiate treeing through electron avalanching.

FEP had generally higher initiation voltage and time, as well as slower tree propagation, while also having the highest level of PD activity. While the tree propagation for the majority of FEP samples appeared to occur in stages, PD activity increased steadily throughout the test period and is therefore likely related to the increase in number and thickness of the tree channels closer to the needle tip rather than the lead channels. Also, for PFA there are indications of this, as the PD activity increases steadily throughout the test while the tree growth rate varies. It has the lowest PD level of all three materials but has a higher average growth rate than FEP.

With regards to tree morphology, the size of the tree does not appear to affect the growth rate for XLPE: all trees propagate with a relatively constant growth rate regardless of how much of the gap the tree has covered. This is not the case for FEP, where for the majority of samples, the tree propagation slowed down or paused at approximately 50-60 % of the gap distance. This is where the electric field in a non-treed sample would be the lowest (Fig. 1). A drop-off in growth rate would therefore be expected as there would be less energy to break polymer bonds. With insulating tree channels there might also be some screening of the needle, but it would be expected to be significantly less than for conductive channels. In PFA, the reduction in tree growth rate occurs at different percentages of gap distances being covered by the electrical tree, reducing the likelihood that it is a reduction of the electric stress only caused by the original electrode geometry.

IV. Conclusion

Electrical treeing in PFA and FEP was found to occur at a slower propagation rate than for XLPE. FEP had the highest PD activity and the slowest propagation rate, while PFA had the lowest PD activity and intermediate propagation rate. It is suspected that the reduced growth rate and increased tree initiation time are related to the higher bond strength of FEP and PFA making it harder for autooxidation to take place. Both fluoropolymers grew bushy trees, with FEP trees being slightly broader and having a higher density of channels, while in XLPE the trees were bush-branched. The PD activity in all materials were consistent with insulating tree channels, which also would explain a stagnation in tree propagation observed for FEP and PFA. Post-breakdown, there were indications of conductive byproducts being present, as the breakdown channel in all three materials appeared black and traces of carbonaceous compounds were found by Raman spectroscopy in all three materials.

References

[1] B. Johnson, R. Barth, P. House, and J. Kuntscher, 'Controlling pipe and equipment operating temperatures with trace heating systems', in *PCIC Europe 2013*, May 2013, pp. 1–10.
[2] N. Shimizu and C. Laurent, 'Electrical tree initiation', *IEEE Transactions on Dielectrics and Electrical Insulation*, vol. 5, no. 5, pp. 651–659, Oct. 1998, doi: 10.1109/94.729688.
[3] X. Zheng and G. Chen, 'Propagation mechanism of electrical tree in XLPE cable insulation by investigating a double electrical tree structure', *IEEE Transactions on Dielectrics and Electrical Insulation*, vol. 15, no. 3, pp. 800–807, Jun. 2008, doi: 10.1109/TDEI.2008.4543118.
[4] B. R. Varlow and D. W. Auckland, 'Mechanical aspects of electrical treeing in solid insulation', *IEEE Electrical Insulation Magazine*, vol. 12, no. 2, pp. 21–26, Apr. 1996, doi: 10.1109/57.486948.
[5] M. A. Baferani, C. Li, T. Shahsavarian, J. Ronzello, and Y. Cao, 'High temperature insulation materials for DC cable insulation—Part I: space charge and conduction', *IEEE Transactions on Dielectrics and Electrical Insulation*, vol. 28, no. 1, pp. 223–230, 2021.
[6] T. Shahsavarian *et al.*, 'High temperature insulation materials for DC cable insulation—Part II: Partial discharge behavior at elevated altitudes', *IEEE Transactions on Dielectrics and Electrical Insulation*, vol. 28, no. 1, pp. 231–239, 2021.
[7] C. Li, T. Shahsavarian, M. A. Baferani, N. Wang, J. Ronzello, and Y. Cao, 'High temperature insulation materials for DC cable insulation—Part III: Degradation and surface breakdown', *IEEE Transactions on Dielectrics and Electrical Insulation*, vol. 28, no. 1, pp. 240–247, 2021.
[8] L. A. Dissado and J. C. Fothergill, *Electrical degradation and breakdown in polymers*, 1st ed. in IEEE materials and devices, no. 9. London: Peter Peregrinus Ltd., 1992.
[9] N. Shimizu and H. Tanaka, 'Effect of liquid impregnation on electrical tree initiation in XLPE', *IEEE Transactions on Dielectrics and Electrical Insulation*, vol. 8, no. 2, pp. 239–243, 2001.
[10] I. Gallimberti, 'The mechanism of the long spark formation', *Le Journal de Physique Colloques*, vol. 40, no. C7, pp. C7-193, 1979.
[11] T. L. Cottrell, 'The strengths of chemical bonds', *(No Title)*, 1954.
[12] E. Giannetti, 'Semi-crystalline fluorinated polymers', *Polymer international*, vol. 50, no. 1, pp. 10–26, 2001.
[13] P. Kelleher, 'Thermal oxidation of thermoplastics', *Journal of Applied Polymer Science*, vol. 10, no. 6, pp. 843–857, 1966.
[14] X. Chen, Y. Xu, X. Cao, S. Dodd, and L. Dissado, 'Effect of tree channel conductivity on electrical tree shape and breakdown in XLPE cable insulation samples', *IEEE Transactions on Dielectrics and Electrical Insulation*, vol. 18, no. 3, pp. 847–860, 2011.
[15] G. Chen and C. H. Tham, 'Electrical treeing characteristics in XLPE power cable insulation in frequency range between 20 and 500 Hz', *IEEE Transactions on Dielectrics and Electrical Insulation*, vol. 16, no. 1, pp. 179–188, Feb. 2009, doi: 10.1109/TDEI.2009.4784566.
[16] H. Ichikawa, Y. Suzuoki, T. Mizutani, and K. Uchida, 'Partial discharge patterns of electrical treeing in polyethylene', *Proceedings of 1994 4th International Conference on Properties and Applications of Dielectric Materials (ICPADM)*, vol. 1, pp. 379–382, 1994.
[17] K. Wu, Y. Suzuoki, T. Mizutani, and H. Xie, 'A novel physical model for partial discharge in narrow channels', *IEEE transactions on dielectrics and electrical insulation*, vol. 6, no. 2, pp. 181–190, 1999.
[18] L. A. Dissado, 'Understanding electrical trees in solids: from experiment to theory', *IEEE Transactions on Dielectrics and Electrical Insulation*, vol. 9, no. 4, pp. 483–497, Aug. 2002, doi: 10.1109/TDEI.2002.1024425.
[19] A. S. Vaughan, S. J. Dodd, and S. J. Sutton, 'A Raman microprobe study of electrical treeing in polyethylene', *Journal of materials science*, vol. 39, pp. 181–191, 2004.
[20] H. Zheng, G. Chen, and S. M. Rowland, 'The influence of AC and DC voltages on electrical treeing in low density polyethylene', *International Journal of Electrical Power & Energy Systems*, vol. 114, 2020.
[21] D. A. Bower and W. F. Maddams, *The vibrational spectroscopy of polymers*. 1989.